



ELSEVIER

Biophysical Chemistry 87 (2000) 73–84

Biophysical
Chemistry

www.elsevier.nl/locate/bpc

Fluorescence dynamics of green fluorescent protein in AOT reversed micelles

Marsha A. Uskova^{a,b}, Jan-Willem Borst^a, Mark A. Hink^a,
Arie van Hoek^a, Arjen Schots^c, Natalia L. Klyachko^b,
Antonie J.W.G. Visser^{a,*}

^a*MicroSpectroscopy Centre, Department of Biomolecular Sciences, Wageningen University, Dreijenlaan 3, 6703 HA Wageningen, The Netherlands*

^b*Department of Chemical Enzymology, Faculty of Chemistry, Moscow State University, Moscow 119899 GSP, Russia*

^c*Laboratory for Monoclonal Antibodies, Department of Plant Sciences, Wageningen University, Binnenhaven 12, 6709 PD Wageningen, The Netherlands*

Received 4 November 1999; received in revised form 10 July 2000; accepted 10 July 2000

Abstract

We have used the enhanced green fluorescent protein (EGFP) to investigate the properties of surfactant-entrapped water pools in organic solvents (reversed micelles) with steady-state and time-resolved fluorescence methods. The surfactant used was sodium bis(2-ethylhexyl)sulfosuccinate (AOT) and the organic solvents were isooctane and (the more viscous) dodecane, respectively. The water content of the water pools could be controlled through the parameter w_0 , which is the water-to-surfactant molar ratio. With steady-state fluorescence, it was observed that subtle fluorescence changes could be noted in reversed micelles of different water contents. EGFP can be used as a pH-indicator of the water droplets in reversed micelles. Time-resolved fluorescence methods also revealed subtle changes in fluorescence decay times when the results in bulk water were compared with those in reversed micelles. The average fluorescence lifetimes of EGFP scaled with the relative fluorescence intensities. Time-resolved fluorescence anisotropy of EGFP in aqueous solution and reversed micelles yielded single rotational correlation times. Geometrical considerations could assign the observed correlation times to dehydrated protein at low w_0 and internal EGFP rotation within the droplet at the highest w_0 . © 2000 Published by Elsevier Science B.V. All rights reserved.

Keywords: Green fluorescent protein; Reversed micelles; AOT; Water droplets; Time-resolved fluorescence

* Corresponding author. Tel.: +31-317-482862; fax: +31-317-484801.

E-mail address: ton.visser@laser.bc.wau.nl (A.J. Visser).

1. Introduction

The green fluorescent protein (GFP) from the jellyfish *Aequorea victoria* has received widespread utilization as a natural fluorescent marker for gene expression and the localization of gene products [1,2]. The chemical structure of the hexapeptide chromophore has been elucidated [3]. A comprehensive review of all properties of GFP and its numerous bright mutants as well as their applications has been recently published [4]. The fluorescence dynamics of wild-type GFP have been studied with ultra-fast optical spectroscopic techniques [5,6]. Multiple conformational states were identified, which may interconvert slowly in the ground state, but very rapidly in the excited state. A distinct deuterium isotope effect strongly suggests that these states involve a proton transfer reaction. A reaction scheme of two ground states, two excited states and a putative intermediate state has been derived, consistent with these observations [5]. The two ground states are designated A, absorbing at 395 nm, and B, absorbing at 475 nm. The two excited states are A^* , which is protonated, and B^* , which is deprotonated. The intermediate state I^* has a lower energy than A^* , is like B^* deprotonated and forms the linkage between A^* and B^* . Both B^* and I^* emit green fluorescence with an emission maximum at 507 nm. The structural basis for such a reaction scheme has been provided by a 2.1-Å resolution crystal structure [7]. The existence of the three-level scheme has been further validated by low-temperature hole-burning experiments [8], in which slightly different energies of the I^* and B^* states have been identified. Quantum chemical calculations have also inferred a dark zwitterionic state [9], which communicates with the B state and is involved with the blinking behavior of GFP (and other variants) as observed with single-molecule fluorescence detection techniques [10,11]. Other crystallographic 3D-structures, also from GFP mutants, have also been reported [12–14]. Many GFP mutants with distinct spectral properties have been created nowadays (see [4]). For the purpose of this investigation, we have prepared a red-shifted mutant by mutating Phe 64 to Leu

and Ser 65 to Thr, which shows one prominent excitation peak at 489 nm arising from the B conformation. This is the so-called enhanced green fluorescent protein (EGFP). The fluorescence maximum is located at 510 nm. The fluorescence of this mutant EGFP shows a distinct pH dependence, having the largest fluorescence quantum yield at higher pH (pH 9–11) and a progressive decrease in fluorescence at lower pH values until approximately pH 3–4, where the emission is strongly quenched [15,16]. The cause for the drop in fluorescence is the generation of a non-fluorescent (at 409 nm excitation) protonated form of the chromophore in the protein environment with a distinct pK_a value. In this way, EGFP has been proposed as an intracellular pH indicator [15,17].

In the crystal structure of GFP, the fluorophore is part of a central helix inside a 11-stranded β -barrel. The hexapeptide is, therefore, buried in the protein matrix and is highly protected from bulk solvent by the surrounding β -strands. From time-resolved fluorescence anisotropy of EGFP, which reports on the rotational properties, it was demonstrated that the fluorophore does not show any internal motion on the fluorescence time scale and, therefore, registers only protein rotation [18–20]. The strong fluorescence of the rigidly bound hexapeptide has prompted us to use EGFP as a model protein to investigate its physico-chemical properties in reversed micelles. Reversed micelles are tiny water droplets surrounded by a monolayer of surfactant molecules and dispersed in a water-immiscible organic solvent [21]. Reversed micelles have been used as an important research tool in the field of micellar enzymology [22,23]. Since proteins in reversed micelles are optically transparent, fluorescence spectroscopy has been proven to be a convenient method to characterize the dynamic structure around given fluorophores in proteins [24,25]. These media have the additional advantage that the water content, and, therefore, the protein hydration level, can be controlled through the parameter w_0 , which is the water-to-surfactant molar ratio. We have chosen the well-studied sodium bis(2-ethylhexyl)sulfosuccinate (AOT) as a surfactant for reversed micelles. The aim of this

study was to answer the following questions: (i) does the dynamic behavior of EGFP change at various w_0 -values? (ii) Is the pH inside the water droplet the same as the pH in bulk water? The use of indicator dyes and ions have led to ambiguous pH-values because of interactions between these reporter molecules and the surfactant interface (see Section 4). Such problems can be circumvented by using EGFP as an indicator protein. (iii) Does the volume of the EGFP-containing water droplets change with increasing w_0 and can protein rotation inside the droplet be observed? This aspect has been investigated previously with proteins of similar and larger size (see Section 4). EGFP has the distinct advantage that the fluorescence anisotropy decays as a rigid rotor without any rapid internal protein motion, enabling a more direct interpretation of the results.

2. Materials and methods

EGFP was expressed in *E. coli* bacteria (XL1-Blue-MRF⁺ Kan, Stratagene). Proteins were extracted using the French pressure method and the (His)₆-tagged soluble EGFP was purified via Ni-NTA affinity chromatography. Bound proteins were eluted with a 250-mM imidazole buffer and the fraction was concentrated with a Millipore YM 10 spin concentrator. The concentrated fraction was applied on a Superdex PG 200 gel filtration column for further purification, and the final preparation was essentially pure, as demonstrated by coomassie-stained polyacrylamide gel. Aliquots (10 μ l) of 26 μ M EGFP in a final buffer of 20 mM Tris-HCl (pH 8.2) 120 mM KCl were stored at -20°C . AOT was obtained from Sigma (St. Louis, MO, USA). Except for pH-dependent experiments, EGFP was stored in 20 mM Tri-HCl buffer, pH 8.2. Water was purified on a Millipore system. Isooctane and dodecane were from Sigma and used as received. Reversed micelles were prepared by adding 2 μ l of the EGFP stock solution and a previously determined volume of buffer (to reach the desired w_0) to 1 ml of 100 mM AOT in organic solvent (either isooctane or

dodecane). The mixture was gently shaken until a clear solution was obtained. To obtain samples with higher water content, a predetermined amount of buffer was added to the same sample and the mixture was shaken again. The total concentration of EGFP in reversed micelles was always the same as the corresponding EGFP in buffer solution. The following buffers were used for the pH-dependent studies (molarity was always 20 mM): sodium citrate for pH 4 and 5, potassium phosphate for pH 6, 7 and 8, sodium borate for pH 9 and sodium carbonate-bicarbonate for pH 10 and 11.

The steady-state fluorescence spectra were obtained with a Spex-Fluorolog 3.2.2 spectrofluorometer. The monochromator slit widths were 1 nm in excitation and 2 nm in emission. The emission spectra were corrected for the spectral characteristics of emission monochromator and photomultiplier. The spectra of buffer or solvent were also collected under the same conditions and subtracted from the corresponding fluorescence spectra. Time-resolved polarized fluorescence experiments were carried out using a picosecond laser system and time-correlated single photon counting, as described in detail elsewhere [26–29]. The excitation wavelength was 450 nm (stilbene dye as laser medium, pumped by a mode-locked Nd-YLF laser) and the fluorescence was selected by using two KV500 cut-off filters (Schott, Mainz, Germany). The time equivalence per channel in the multichannel analyzer was 5.24 ps and decay curves were collected in 4000 channels. The fluorescence decay experiments were analyzed according to a multi-exponential decay law (three lifetimes (τ_i) and three amplitudes (α_i); $i = 1, 3$) using a global analysis program, whose principle has been described previously [30] and which is based on a Marquardt non-linear least squares procedure [31]. The average lifetime $\langle\tau\rangle$ has been calculated as $\sum\alpha_i\tau_i$, in which the sum of the amplitudes has been normalized to unity. The fluorescence anisotropy decay was globally analyzed with a mono-exponential decay law.

All experiments were conducted at room temperature (22°C).

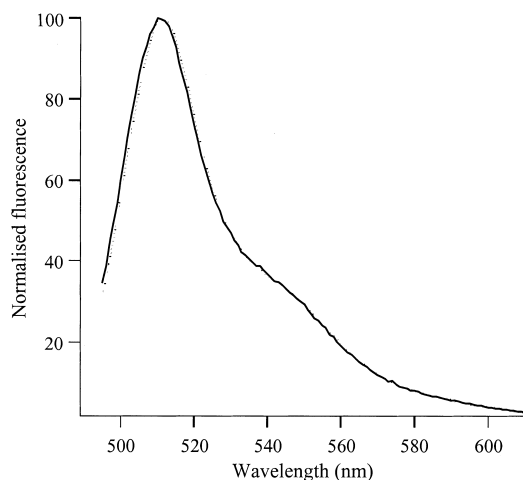


Fig. 1. Fluorescence spectra of EGFP in 20 mM Tris buffer, pH 8.2 (solid line) and of EGFP in AOT reversed micelles in isooctane at $w_0 = 8$ (dotted line) (the water droplets contain the same buffer as used for the bulk). The spectra are normalized and overlaid for clarity.

3. Results

3.1. Steady-state fluorescence spectra of EGFP

Examples of fluorescence spectra of EGFP in buffer and AOT reversed micelles (isooctane, $w_0 = 8$) are given in Fig. 1. The normalized spectra can be overlaid, implying that there was no shift in the emission maximum. Instead of using integrated emission spectra, the relative fluorescence yield could then be expressed by the relative fluorescence intensity maximum (the EGFP concentration was always the same). The relative fluorescence intensity maxima showed a dependence on w_0 , which is illustrated in Fig. 2 for EGFP in AOT reversed micelles in two different organic solvents (isooctane and dodecane). When the water content was low ($w_0 < 4$), the fluorescence intensity of EGFP was lower than in aqueous buffer. The effect was much more pronounced for reversed micelles with dodecane as the organic phase.

The EGFP fluorescence spectra have been investigated in AOT reversed micelles in isooctane with different water contents and at different pH values. The relative fluorescence intensity maxima (relative to the values at pH 11) of EGFP as

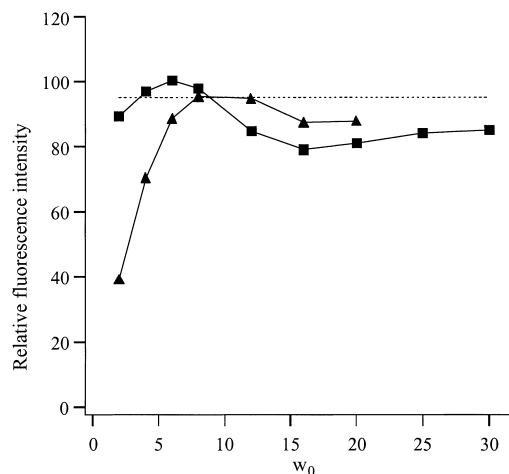


Fig. 2. Dependence of the maximum intensity of the EGFP-fluorescence on the water content of AOT reversed micelles in isooctane (■) and dodecane (▲). The dashed line represents the fluorescence intensity of EGFP in water.

function of pH have been given in Fig. 3 for AOT reversed micelles (at three different water con-

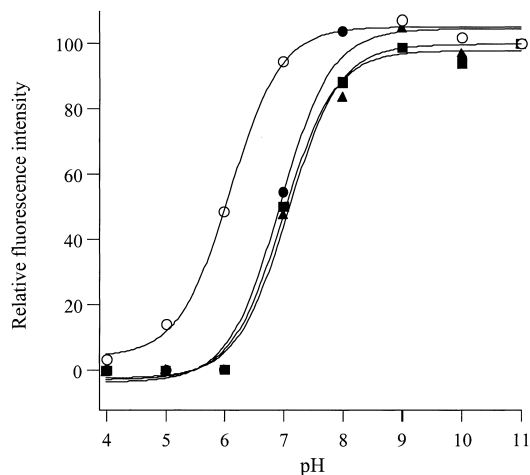


Fig. 3. The pH-dependence of the fluorescence intensity of EGFP in aqueous buffer solutions and in AOT reversed micelles in isooctane at $w_0 = 4, 13$ and 25 . The data points are normalized to the intensities obtained at pH 11. The lines through the intensity points (I) is a fit to the equation $I = A + B / \{1 + 10^{(pK_a - pH)}\}$ where A and B are related to the offset and maximum range of the data (see [15,17]). The optimized values are for aqueous buffer (○) $pK_a = 6.1 \pm 0.1$ and water pools of $w_0 = 4$ (■) $pK_a = 7.1 \pm 0.1$; $w_0 = 13$ (●) $pK_a = 6.9 \pm 0.1$; $w_0 = 25$ (▲) $pK_a = 7.0 \pm 0.1$.

Table 1
Fluorescence decay parameters of EGFP in aqueous buffer and in AOT/isooctane reversed micelles of different water content^{a,b,c}

Parameter	Buffer	$w_0 = 2$	$w_0 = 4$	$w_0 = 6$	$w_0 = 8$	$w_0 = 12$	$w_0 = 16$	$w_0 = 20$	$w_0 = 25$	$w_0 = 30$
α_1	0.12	0.10	0.08	0.10	0.12	0.11	0.11	0.10	0.08	0.10
τ_1 , ns	0.11 (0.02–n.d.)	0.19 (0.04–n.d.)	0.25 (0.03–n.d.)	0.27 (0.08–n.d.)	0.21 (0.09–n.d.)	0.23 (0.08–n.d.)	0.15 (0.03–n.d.)	0.16 (0.03–n.d.)	0.20 (0.006–n.d.)	0.40 (0.1–0.53)
α_2	0.14	0.18	0.16	0.19	0.18	0.23	0.17	0.17	0.16	0.31
τ_2 , ns	1.26 (0.87–2.23)	1.26 (0.85–2.12)	1.24 (0.79–n.d.)	1.40 (0.91–2.24)	1.32 (0.9–2.33)	1.38 (0.97–2.18)	1.19 (0.92–2.15)	1.16 (0.81–2.02)	1.17 (0.78–n.d.)	1.90 (0.92–2.41)
α_3	0.74	0.72	0.76	0.71	0.70	0.66	0.72	0.73	0.76	0.59
τ_3 , ns	2.81 (2.78–3.01)	2.58 (2.54–2.85)	2.57 (2.54–3.12)	2.58 (2.5–3.04)	2.56 (2.45–3.5)	2.56 (2.51–3.08)	2.52 (2.5–2.76)	2.52 (2.49–2.72)	2.53 (2.5–3.37)	2.70 (2.64–3.45)
$\langle \tau \rangle$, ns	2.27	2.09	2.18	2.14	2.06	2.03	2.02	2.04	2.12	2.22

^aDecay analysis was performed using a sum of three exponentials [amplitudes α_i and lifetimes τ_i ($i = 1,3$)].

^bThe values within parentheses are the confidence limits taken at the 67% level.

^cn.d. = not defined.

Table 2
Fluorescence decay parameters of EGFP in aqueous buffer and in AOT/dodecane reversed micelles of different water content^{a,b,c}

Parameter	Buffer	$w_0 = 2$	$w_0 = 4$	$w_0 = 6$	$w_0 = 8$	$w_0 = 12$	$w_0 = 16$	$w_0 = 20$	$w_0 = 21.7$	$w_0 = 23.3$
α_1	0.12	0.18	0.11	0.10	0.11	0.10	0.11	0.10	0.11	0.11
τ_1 , ns	0.11 (0.02–n.d.)	0.09 (0.04–n.d.)	0.31 (0.03–0.67)	0.36 (n.d.–0.75)	0.37 (n.d.–n.d.)	0.40 (n.d.–0.8)	0.43 (0.12–0.72)	0.11 (0.07–n.d.)	0.44 (0.13–0.65)	0.39 (0.04–0.7)
α_2	0.14	0.15	0.14	0.13	0.11	0.12	0.27	0.13	0.35	0.19
τ_2 , ns	1.26 (0.87–2.23)	0.93 (0.67–n.d.)	1.41 (0.61–2.43)	1.50 (0.67–n.d.)	1.50 (n.d.–n.d.)	1.42 (n.d.–n.d.)	1.84 (1.3–2.4)	0.89 (0.58–n.d.)	1.98 (0.74–2.38)	1.64 (0.7–2.41)
α_3	0.74	0.67	0.75	0.77	0.78	0.78	0.62	0.77	0.54	0.70
τ_3 , ns	2.81 (2.78–3.01)	2.48 (2.46–3.65)	2.50 (2.46–3.37)	2.49 (1.48–3.27)	2.47 (0.97–3.21)	2.47 (2.38–3.29)	2.55 (2.46–n.d.)	2.42 (2.38–3.37)	2.58 (2.43–n.d.)	2.50 (2.43–3.62)
$\langle \tau \rangle$, ns	2.27	1.83	2.11	2.14	2.14	2.13	2.11	2.01	2.12	2.11

^aDecay analysis was performed using a sum of three exponentials [amplitudes α_i and lifetimes τ_i ($i = 1,3$)].

^bThe values within parentheses are the confidence limits taken at the 67% level.

^cn.d. = not defined.

tents) and for the bulk water. The shape of the curves was similar for reversed micellar and water solutions, but there was a distinct shift to alkaline pH in reversed micelles, irrespective of water content. The transition midpoint was at pH 6.1 in aqueous solution, while the midpoints were shifted to pH 7.0 for reversed micelles. A midpoint at pH 5.8–6.0 for EGFP in water was also found by Kneen et al. [15] and Robey et al. [17]. The shift in pH values in reversed micelles may well be due to differences in pH between the water droplet and bulk water.

3.2. Time-resolved fluorescence of EGFP

Typical experimental and fitted fluorescence decay curves of EGFP in aqueous and reversed micellar solution (AOT/isooctane, $w_0 = 8$) are presented in Fig. 4. A minimum decay model for an adequate approximation consists of a sum of three exponential components. All parameters [pre-exponential factors α_i and fluorescence lifetimes τ_i ($i = 1,3$)] for both types of reversed micelles having different water contents are collected in Table 1 (AOT reversed micelles in isooctane) and Table 2 (AOT reversed micelles in dodecane). For easy comparison, the average fluorescence lifetime $\langle\tau\rangle$ is also presented in Tables 1 and 2. The most dominant lifetime component of EGFP in buffer was the longest one of 2.8 ns. Significant, but minor contributions of lifetimes of 0.11 and 1.2 ns are also present. When we compared these fluorescence lifetime components in reversed micelles, the following trends could be seen: the 0.11-ns component became longer and the 2.8-ns component became shorter in reversed micelles. The lifetime of 1.2 ns seems to be less sensitive, although the values were scattered. The average fluorescence lifetime $\langle\tau\rangle$ was shorter in reversed micelles. The largest effect was seen for EGFP in AOT/dodecane at $w_0 = 2$, in full agreement with the relatively large decrease in fluorescence intensity.

3.3. Fluorescence anisotropy decay of EGFP

Examples of experimental and fitted fluorescence anisotropy decays are presented in Fig. 5

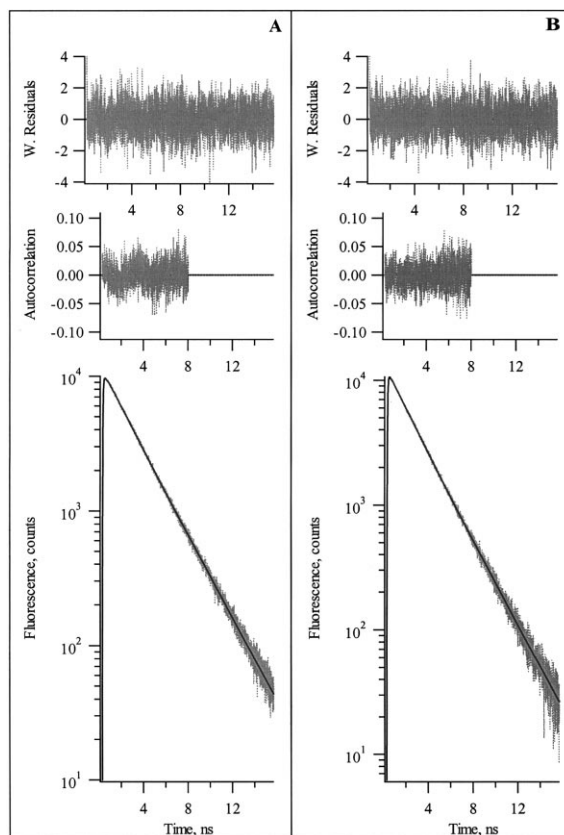


Fig. 4. Examples of experimental (dotted line) and fitted (solid line) fluorescence decay curves of EGFP in 20 mM Tris-HCl buffer, pH 8.2 (panel A) and of EGFP in AOT reversed micelles in isooctane at $w_0 = 8$ (same buffer as in A) (panel B). Optimized parameter values [amplitudes α_i and lifetimes τ_i ($i = 1,3$)] are listed in Table 1. Residuals and autocorrelation traces of the residuals are presented to illustrate the good quality of the fits.

for EGFP in water and in reversed micelles (AOT/isooctane, $w_0 = 8$). A single rotational correlation time gave a good fit to the data in all cases. The single correlation time reflected the rotation of the protein as a whole or, in case of reversed micelles, the (hydrated) protein, surrounded by a shell of surfactants. There was no sign of independent rotation of the fluorophore inside the protein matrix, which was a conclusion previously reached by the authors [18,19] and by others [20,32]. Another feature was the high initial anisotropy (the average value of all experi-

ments was 0.385), which indicated that the angle between absorption and emission transition moment was small [18]. A summary of all the results is given in Fig. 6. In both AOT reversed micelles, it was clear that the correlation time depended on the water content. The shortest correlation time was found at $w_0 = 2$, then there was a small increase until a maximum correlation time was reached, which was followed by a decrease in correlation time at larger w_0 values. The latter effect was clearer for EGFP in AOT/dodecane reversed micelles, in which the longer correlation time was due to the higher viscosity of dodecane ($\eta = 1.35$ cP at 25°C) [33] as compared to isooctane ($\eta = 0.474$ cP at 25°C) [34]. The shorter rotational correlation times observed at low water content could be explained by the incomplete hydration of EGFP. After hydration of the protein, the reversed micelles expand and the maximum size is reached before the protein can independently rotate inside the droplet (for AOT/dodecane this is at $w_0 = 8$, and for AOT/isooctane at $w_0 = 12$ –20). The further decrease of the apparent rotational correlation time at high water content arose from contributions of overall droplet rotation and internal motion, as similarly observed for alcohol dehydrogenase [35].

4. Discussion

4.1. Steady state fluorescence experiments

The first observation was the diminished fluorescence of EGFP in water pools containing a minimum amount of water (see Fig. 2). It is known that at small values of w_0 , all water molecules are used for hydrating the polar surfactant head groups [36]. Therefore, EGFP seems to be less hydrated in reversed micelles of low water content, which is manifested by an altered microenvironment near the fluorophore. There are a number of polar groups and structured water molecules located in the immediate vicinity of the fluorophore participating in a hydrogen bonding network, which can act in synergy as an efficient charge-relay system [12]. On the basis of the three-dimensional structure, it has been proposed

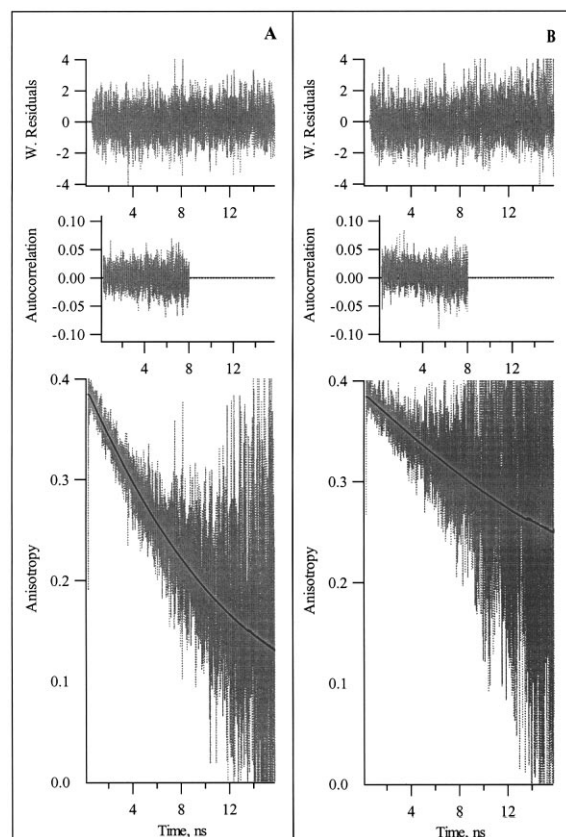


Fig. 5. Examples of experimental (dotted curve) and fitted (solid line) fluorescence anisotropy decay curves of EGFP in 20 mM Tris-HCl buffer, pH 8.2 (panel A) and of EGFP in AOT reversed micelles in isooctane at $w_0 = 8$ (same buffer as in A) (panel B). The optimized parameter values are $\phi = 13.5$ ns and $\beta = 0.385$ for EGFP in water and $\phi_{\text{mic}} = 33$ ns and $\beta = 0.385$ for EGFP in reversed micelles. Residuals and autocorrelation traces of the residuals are presented to illustrate the good quality of the fits.

that Glu 222 plays a pivotal role as an acceptor in the excited-state proton transfer (ESPT) mechanism [5,7], although FTIR difference spectra indicate that this residue is deprotonated in both A and B forms [37]. It is very well conceivable that the ionization of the fluorophore is somewhat influenced by a slightly altered solvation, leading to diminished fluorescence.

EGFP in reversed micelles shows the same distinct pH-dependence of the fluorescence as EGFP in bulk solution, but the curves are dis-

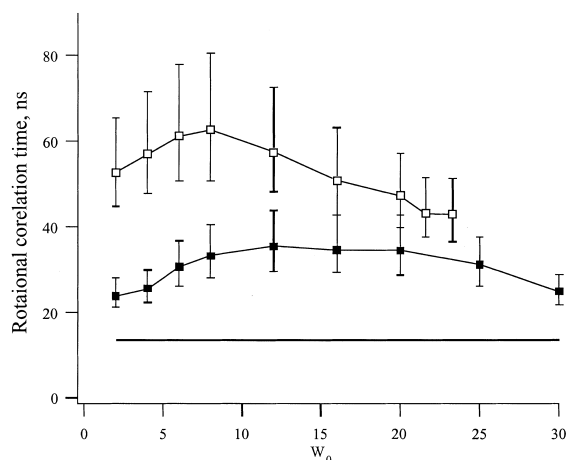


Fig. 6. Rotational correlation times of EGFP in AOT reversed micelles in isooctane (■) and dodecane (□) at different w_0 values and in water (—). The buffer used was 20 mM Tris-HCl buffer, pH 8.2. The error bars represent the recovered confidence limits at the 66% level (for details see [30]).

placed over one pH unit, irrespective of the water content (see Fig. 3). The acidities of surfactant-entrapped water pools have been assessed either by titrating solubilized dyes [38] or by measuring the ^{31}P (NMR) chemical shifts of phosphate buffers in water pools relative to those in bulk water [39]. The disadvantage of using dyes is the fact that they are charged and can be adsorbed to the surfactants, which drastically influences the apparent $\text{p}K_a$ value of the dye. In addition, certain buffers can displace the dye molecule from the surfactant binding site, thereby immediately changing the apparent $\text{p}K_a$ value [33]. The combination of ^{31}P chemical shifts and the use of indicator dyes in AOT-entrapped water pools led Smith and Luisi [39] to conclude that these dyes have limited use for determining an acidity scale in reversed micelles. The advantage of using EGFP is the fact that the fluorophore is buried in the protein matrix and is not in direct contact with buffer ions or charged surfactants. Protonation of the hydroxyl group of the Tyr-66 part of the fluorophore is responsible for the fluorescence quenching and gives rise to a $\text{p}K_a$ value of approximately 6 [16]. This effect is largely induced by the concentration of protons present in the external water. For this reason we believe that

EGFP is a better pH-indicator than most pH sensitive dye molecules used thus far. The apparent shift of pH to higher values in the AOT-enclosed water droplets can be explained by the potential field of the negatively charged surfactant, which attracts protons from the interior of the droplet.

4.2. Time-resolved fluorescence

The fluorescence decay of EGFP both in bulk water and surfactant-enclosed water droplets is clearly heterogeneous (see Fig. 4 and Tables 1 and 2). The longest fluorescence decay component of EGFP in bulk water is 2.8 ns and is the predominant one. This component very likely arises from the deprotonated state B^* . The shorter lifetime components must be associated with the emissive properties of the intermediate (deprotonated) state I^* and the protonated state A^* . The intermediate state I^* is assigned to the lifetime component of 1.2 ns, since I^* is an unrelaxed form of B^* and, therefore, shorter-lived than B^* . On the other hand, I^* is generated via ESPT from state A^* and is, therefore, longer-lived than A^* , since an uphill back transfer from I^* to A^* is unlikely. It is very possible that the excitation wavelength used (450 nm) still excites a minor amount of the protonated form A, whose fluorescence competes with ESPT, giving rise to the presence of a small fraction of the shortest component of 0.11 ns. Given the complexity of the proposed three-level (and even four-level [8]) schemes, it is difficult to imagine that single exponential fluorescence decays have been found for EGFP and other variants [11,20]. The changed properties of the surfactant-encapsulated water droplets, as compared to bulk water, may be the reason for the slightly altered fluorescence decay times of EGFP in reversed micelles. The hydrogen bonding network involving the bound water can undergo some subtle changes, which is reflected in a change in ESPT- and other kinetic rate constants connected to the complex three-level scheme describing the fluorescence decay kinetics of EGFP. Changes in rate constants are then manifested by changes in fluorescence lifetimes and pre-exponential factors. The shorter

average fluorescence lifetimes are in agreement with the decreased relative fluorescence intensities (see Fig. 2).

4.3. Time-resolved fluorescence anisotropy

Analysis of the fluorescence anisotropy decays (Figs. 5 and 6) provides evidence that the global rotation of EGFP in different media is observed. In aqueous solution, the recovered rotational correlation time was characteristic for the rotation of the hydrated protein in water. In reversed micelles, the rotational correlation time (ϕ_{mic}) reflected the rotation of the protein surrounded by water and a monolayer of hydrated surfactant. Since the data were obtained with sufficient precision (see Fig. 6), we can draw some important conclusions. In reversed micelles, there are two regimes. The first regime is at low water content ($w_0 < 5$) where the rotational correlation times of EGFP are distinctly shorter, irrespective of the organic solvent. In this regime, the water is used for hydrating the surfactant, leading to a less hydrated protein. Similar results were obtained with a fluorescent derivative of α -chymotrypsin in AOT reversed micelles [24]. Increasing the water content will hydrate EGFP and expand the rotating unit. The second regime is at high water content, where an increase in w_0 leads to a progressively shorter rotational correlation time. The onset of the latter regime depends on the choice of organic solvent. The range is $w_0 = 8\text{--}23$ for EGFP in AOT/dodecane and $w_0 = 15\text{--}30$ in

AOT/isooctane. The apparent shortening of the rotational correlation time at increasing w_0 has also been observed previously for alcohol dehydrogenase in AOT reversed micelles in isooctane [35].

We have calculated the hydrodynamic radii (R_h) of EGFP in reversed micelles at low water content ($w_0 = 2\text{--}8$) from the Stokes–Einstein relation for spherical particles:

$$\phi = \frac{4\pi R_h^3 \eta}{3kT} \quad (1)$$

T is the absolute temperature and k is the Boltzmann constant. The solvent viscosities (η) used were the ones at 298 K (vide supra), but this gives only a minor deviation from the actual viscosities at the measurement temperature (295 K). The radius of the inner cavity (R_{ic}) is then calculated as the difference between the hydrodynamic radius and the length of a single AOT molecule (1.2 nm, [40]). For calculations of the aggregation number (n), a value of 0.55 nm² was used as the surface area of the polar head of one AOT molecule [40]. From geometric considerations n can be determined from:

$$n = \frac{4\pi R_h^2}{0.55} \quad (2)$$

All results for low water content are listed in Table 3. The difference in hydrodynamic radii between the hydrated EGFP and the less hy-

Table 3

Rotational correlation times (ϕ_{mic}), micellar radii (R_h and R_{ic}) and aggregation numbers (n) of EGFP-loaded AOT reversed micelles in isooctane and dodecane at relatively low w_0

w_0	Solvent	ϕ_{mic} , (ns)	R_h , (nm)	R_{ic} , (nm)	n
2	isooctane	23.7	3.64	2.44	302
4	isooctane	25.5	3.73	2.53	318
6	isooctane	30.6	3.96	2.76	358
8	isooctane	33.2	4.08	2.88	380
2	dodecane	52.7	3.37	2.17	259
4	dodecane	57.0	3.46	2.26	273
6	dodecane	60.9	3.54	2.34	286
8	dodecane	62.5	3.57	2.37	291

drated one amounted to 0.4 nm for isooctane and 0.2 nm for the dodecane-solubilized protein (note, however, that in the latter case, the error in the determination of rotational correlation times was larger, see Fig. 6). The thickness of a hydration shell around a globular protein is approximately 0.3 nm, which is equivalent to one layer of water [41]. Therefore, it is very likely that the small increase in the hydrodynamic radius was connected with the hydration of EGFP. The inner radius R_{ic} amounted to 2.1–2.5 nm for EGFP in both types of droplets. This radius was in the range of the one calculated according to Eq. (1) for EGFP in water ($\phi = 13.5$ ns, yielding $R_h = 2.37$ nm). This implied that the data were internally consistent. The surfactant aggregation number varied from 250 to 380 for different types of protein-filled droplets (see Table 3). This number can be expected for reversed micelles having this size [42]. It is, therefore, important to conclude that EGFP creates its own surfactant-stabilized water shell.

The shortening of the rotational correlation time of EGFP in reversed micelles of higher water content can be due to an additional contribution to the anisotropy decay: an increased mobility of the protein within the micelle. The fluorescence anisotropy decay is then determined by two processes (each with its own correlation time): overall rotation of the protein including the droplet (ϕ_{mic}) and the internal motion of the protein inside the droplet (ϕ_{int}). Assuming that these motions are independent, the observed rotational correlation time ϕ_{obs} is related to ϕ_{mic} and ϕ_{int} as follows [35]:

$$\frac{1}{\phi_{obs}} = \frac{1}{\phi_{mic}} + \frac{1}{\phi_{int}} \quad (3)$$

In order to get an idea of the order of magnitude of the correlation time for internal motion, we have to make one crucial assumption. The overall rotational correlation time of the EGFP-filled micelles (ϕ_{mic}) is fixed to its maximum value ($\phi_{mic} = 35$ ns for isooctane and $\phi_{mic} = 62$ ns for dodecane, see Fig. 6). Values are given only for the water pools containing the largest amounts of water: for EGFP in AOT/isooctane/water with

$w_0 = 25$, $\phi_{int} = 250$ ns and with $w_0 = 30$, $\phi_{int} = 80$ ns; for EGFP in AOT/dodecane/water with $w_0 = 20$, $\phi_{int} = 190$ ns and with $w_0 = 23.3$, $\phi_{int} = 135$ ns. From these results it is clear that the internal mobility becomes markedly faster at the highest w_0 indicating that the micelle is somewhat expanded allowing the protein to rotate inside. One should exercise some care, however, in assigning too much value to these numbers after realizing that the time scale of the experiment is only 15 ns, while the recovered internal correlation times are some 10-fold longer.

5. Conclusions

We have demonstrated that EGFP is a sensitive fluorescent indicator protein to measure the acidity scale inside surfactant-encapsulated water droplets. The dynamic fluorescence properties of EGFP are changed in a subtle manner, which is probably related to the different properties of the entrapped water as compared to the bulk water, thereby influencing the hydrogen bonding network near the fluorophore. Analysis of fluorescence anisotropy decay patterns provides us with a powerful tool to derive geometric factors. At low water content, we have proven that EGFP is poorly hydrated, while at high water content the micellar size is such that (hydrated) EGFP is able to rotate within the water droplet.

Acknowledgements

This work was supported by grants from the Technology Foundation and the Council of Earth and Life Sciences of the Netherlands Organization for Scientific Research (NWO), NWO grant 047-007-005 (providing scientific cooperation between The Netherlands and the Russian Federation) and NATO Collaborative Linkage grant CLG 974984.

References

- [1] M. Chalfie, Y. Tu, G. Euskirchen, W. Ward, D. Prasher, *Science* 263 (1994) 802–805.

- [2] P.M. Conn (Ed.), *Methods in Enzymology*, vol. 302. *Green Fluorescent Protein*, Academic Press, San Diego, 1999.
- [3] C.W. Cody, D.C. Prasher, W.M. Westler, F.G. Prendergast, W.W. Ward, *Biochemistry* 32 (1993) 1212–1218.
- [4] R.Y. Tsien, *Ann. Rev. Biochem.* 67 (1998) 509–544.
- [5] M. Chatteraj, B.A. King, G.U. Bublitz, S.G. Boxer, *Proc. Natl. Acad. Sci. USA* 93 (1996) 8362–8367.
- [6] H. Lossau, A. Kummer, R. Heinecke et al., *Chem. Phys.* 213 (1996) 1–16.
- [7] K. Brejc, T.K. Sixma, P.A. Kitts et al., *Proc. Natl. Acad. Sci. USA* 94 (1997) 2306–2311.
- [8] T.M.H. Creemers, A.J. Lock, V. Subramanian, T.M. Jovin, S. Völker, *Nature Struct. Biol.* 6 (1999) 560–567.
- [9] W. Weber, V. Helms, J.A. McCammon, P.W. Langhoff, *Proc. Natl. Acad. Sci. USA* 96 (1999) 6177–6182.
- [10] R.M. Dickson, A.B. Cubbitt, R.Y. Tsien, W.E. Moerner, *Nature* 388 (1997) 355–358.
- [11] P. Schwille, S. Kummer, A.A. Heikal, W.E. Moerner, W.W. Webb, *Proc. Natl. Acad. Sci. USA* 97 (2000) 151–156.
- [12] M. Ormö, A.B. Cubitt, K. Kallio, L.A. Gross, R.Y. Tsien, S.J. Remington, *Science* 273 (1996) 1392–1395.
- [13] F. Yang, L.G. Moss, G.N. Phillips, *Nature Biotechnol.* 14 (1996) 1246–1251.
- [14] G.J. Palm, A. Zdanov, G.A. Gaitanaris, R. Stauber, G.N. Pavlakis, A. Wlodawer, *Nature Struct. Biol.* 4 (1997) 361–365.
- [15] M. Kneen, J. Farinas, Y. Li, A.S. Verkman, *Biophys. J.* 74 (1998) 1591–1599.
- [16] U. Haupts, S. Maiti, P. Schwille, W.W. Webb, *Proc. Natl. Acad. Sci. USA* 95 (1998) 13573–13578.
- [17] R.B. Robey, O. Ruiz, A.V.P. Santoz et al., *Biochemistry* 37 (1998) 9894–9901.
- [18] A.J.W.G. Visser, M.A. Hink, *J. Fluoresc.* 9 (1999) 81–87.
- [19] M.A. Hink, R.A. Griep, J.W. Borst et al., *J. Biol. Chem.* 275 (2000) 17556–17560.
- [20] A. Volkmer, V. Subramanian, D.J.S. Birch, T.M. Jovin, *Biophys. J.* 78 (2000) 1589–1598.
- [21] J.H. Fendler, *Membrane Mimetic Chemistry*, Chapter 3, John Wiley, New York, 1982.
- [22] K. Martinek, A.V. Levashov, N.L. Klyachko, Y.L. Khmel'nitsky, I.V. Berezin, *Eur. J. Biochem.* 155 (1986) 453–468.
- [23] P.L. Luisi, M. Giomini, M.P. Pileni, B.H. Robinson, *Biochim. Biophys. Acta* 947 (1988) 209–246.
- [24] V.N. Dorovska-Taran, C. Veeger, A.J.W.G. Visser, *Eur. J. Biochem.* 211 (1993) 47–55.
- [25] A.J.W.G. Visser, J. van Engelen, N.V. Visser, A. van Hoek, R. Hilhorst, R.B. Freedman, *Biochim. Biophys. Acta* 1204 (1994) 225–234.
- [26] A. van Hoek, A.J.W.G. Visser, *Proc. SPIE* 1640 (1992) 325–329.
- [27] R. Leenders, M. Kooijman, A. van Hoek, C. Veeger, A.J.W.G. Visser, *Eur. J. Biochem.* 211 (1993) 37–45.
- [28] A.J.W.G. Visser, A. van Hoek, N.V. Visser, Y. Lee, S. Ghisla, *Photochem. Photobiol.* 65 (1997) 570–575.
- [29] P.A.W. van den Berg, A. van Hoek, C.D. Walentas, R.N. Perham, A.J.W.G. Visser, *Biophys. J.* 74 (1998) 2046–2058.
- [30] J.M. Beechem, E. Gratton, M. Ameloot, J.R. Knutson, L. Brand, in: J.R. Lakowicz (Ed.), *Topics in Fluorescence Spectroscopy*, vol. 2, Plenum Press, New York, 1991, pp. 241–305.
- [31] D.W. Marquardt, *J. Soc. Ind. Appl. Math.* 11 (1963) 431–441.
- [32] R. Swaminathan, C.P. Hoang, A.S. Verkman, *Biophys. J.* 72 (1997) 1900–1907.
- [33] A.J.W.G. Visser, K. Vos, A. van Hoek, J.S. Santema, *J. Phys. Chem.* 92 (1988) 759–765.
- [34] K. Vos, C. Laane, S.R. Weijers, A. van Hoek, C. Veeger, A.J.W.G. Visser, *Eur. J. Biochem.* 169 (1987) 259–268.
- [35] K. Vos, C. Laane, A. van Hoek, C. Veeger, A.J.W.G. Visser, *Eur. J. Biochem.* 169 (1987) 275–282.
- [36] M. Wong, J.K. Thomas, T. Nowak, *J. Am. Chem. Soc.* 99 (1977) 4730–4736.
- [37] J.J. van Thor, A.J. Pierik, I. Nugteren-Roodzant, A. Xie, K.J. Hellingwerf, *Biochemistry* 37 (1998) 16915–16921.
- [38] F.M. Menger, G. Saito, *J. Am. Chem. Soc.* 100 (1978) 4376–4379.
- [39] R.E. Smith, P.L. Luisi, *Helv. Chim. Acta* 63 (1980) 2302–2311.
- [40] M. Zulauf, H.F. Eicke, *J. Phys. Chem.* 83 (1979) 480–486.
- [41] C.R. Cantor, P.R. Schimmel, *Biophysical Chemistry*, part II, W.H. Freeman, San Francisco, 1980, p. 555.
- [42] R.A. Day, B.H. Robinson, J.H.R. Clarke, J.V. Doherty, *J. Chem. Soc. Faraday Trans.* 75 (1979) 132–139.